

Coulomb-Induced Anomalies in Highly Disordered Superconductors: Application to Tunneling

D. A. Browne,^(a) K. Levin, and K. A. Muttalib^(b)

The James Franck Institute and the Department of Physics, The University of Chicago, Chicago, Illinois 60637

(Received 28 February 1986)

The effects of diffusion-enhanced Coulomb interactions in highly disordered superconductors are studied by use of a set of coupled Eliashberg-type equations in the exact eigenstate representation. Solution of these equations shows how Coulomb-induced inelastic scattering leads to gaplessness and other low-frequency structure in the superconducting state which can be qualitatively correlated with that in the normal density of states. Recent superconducting tunneling experiments compare favorably with this theory.

PACS numbers: 74.60.Mj, 71.55.Jv, 74.50.+r, 74.70.Mq

In the past few years there has been a large effort devoted to an understanding of the interplay of disorder and Coulomb interactions in both the normal and superconducting states. However, previous calculations for the latter have exclusively focused on the behavior of H_{c2} and T_c .^{1,2} Recent superconducting tunneling experiments by Dynes *et al.*³ suggest that valuable information about Coulomb interactions in the presence of strong disorder is contained in the structure of the superconducting density of states $N_s(\omega)$. It is the purpose of the present paper to present a general formulation of the interplay of Coulomb interactions and disorder which can be applied *within* the superconducting state and which treats the normal state on an equivalent footing.

Using the exact-eigenstate⁴ approach and self-consistent Hartree-Fock theory, we derive a set of coupled Eliashberg-type equations for the self-energy. These are then used to compute both the normal and superconducting densities of states. While *self-consistent* Hartree-Fock theory is not a rigorous approach for the

inclusion of higher-order-in- $(1/\varepsilon_F\tau)$ effects, this is the basic framework for treating superconductivity. Furthermore, this approach leads in a more natural way to the same results for the quasiparticle lifetime as have been obtained by previous schemes^{4,5} in which self-consistency was imposed to avoid divergences. Our calculations allow us to extrapolate normal-state properties into the regime of strong disorder where we find considerable deviation from perturbation-theoretic results.

In treating the phonon attraction we, as in all previous studies,^{1,2} rely on earlier calculations⁶ which show that the requirement of charge neutrality cancels the expected enhancement due to the diffusive motion of electrons. By contrast the Coulomb interaction is profoundly affected by disorder and, unlike the phonons, this must be included at the level of a strong-coupling approximation. This is the reverse of the situation in which the standard Eliashberg equations are derived.

With use of the exact-eigenstate basis,⁴ the (matrix) self-consistent Hartree-Fock equations for the Coulomb contribution to the self-energy Σ are

$$\hat{\Sigma}(E, \omega) = -T \sum_{\omega_n'} \sum_q \int dE' V(q, i\omega_n - i\omega_n') L(q, E - E') \tau_3 \hat{G}(E', i\omega_n') \tau_3, \quad (1)$$

where V is the screened Coulomb interaction, G is the matrix Nambu Green's function which depends on Σ , and τ_i are the usual Pauli matrices. The quantity $L(q, E - E')$ is essentially the product of four impurity wave functions and is given phenomenologically in terms of the diffusion constant D by

$$L(q, E - E') = \pi^{-1} (Dq^2) [(E - E')^2 + (Dq^2)^2]^{-1}. \quad (2)$$

We introduce a variational *Ansatz* for the self-energy of the form

$$\hat{\Sigma}(E, i\omega_n) = i\omega_n [1 - Z(E, i\omega_n)] \hat{\tau}_0 - E [1 - Z_3(E, i\omega_n)] \hat{\tau}_3 + [\Phi(E, i\omega_n) - \Phi_0] \hat{\tau}_1. \quad (3)$$

The function $E(1 - Z_3)$ which is usually irrelevant in clean superconductors is important here because of a nonanalytic energy dependence associated with $L(q, E - E')$. Here Φ_0 is the phonon contribution to the pair potential Φ . While our formalism is general our specific calculations will address the 2D limit since there the effects of disorder on the Coulomb interaction are most dramatic. In 3D the singular behavior near the mobility edge is similar to the behavior in 2D in the weakly localized regime.

Detailed examination of Eqs. (1) for real ω shows that because of the singular dependence of the Coulomb kernel at small (E, ω) , the dominant contribution to the integral comes from the energy shell $E' = \omega'$. Because attempts to solve

for the full E and ω dependence proved intractable, Eqs. (1) were solved self-consistently only for the on-shell contributions to $\Sigma(\epsilon, \omega)$, i.e., $\Sigma(\epsilon', \omega') \rightarrow \Sigma(\omega', \omega')$. Our numerical results were checked in the perturbation limit to insure that the functional dependences of Σ found in the above approach agreed with known analytic results.

In our treatment of the superconducting state, we ignore the anomalous pseudopotential effects of the Coulomb interaction.² These can be readily included following Ref. 2. The phonon contribution to the pair potential whose magnitude dominates the Coulomb contribution is given in terms of the BCS coupling constant $N_0 V_{\text{BCS}}$,

$$\Phi_0 = \pi N_0 V_{\text{BCS}} T \sum_{\omega_n'} \frac{1}{Z_3} \frac{\Phi'}{\Omega'}, \quad (4)$$

where $\Omega' = (\omega_n'^2 Z'^2 + \Phi'^2)^{1/2}$ and the primes denote functions of frequency ω_n' . The density of states is obtained from $N(\omega) = \text{Re}(N_0/2\pi i) \text{Tr} \int dE \hat{G}(E, \omega)$ for both the normal (n) and superconducting (s) states.

Equations (1) and (4) were solved numerically on the real axis. In the normal state the weak-scattering limit serves as a useful analytic check on our numerical approximations and gives insight into the self-consistent scheme outlined in Eqs. (1). In this limit that contribution to the normal-state self-energy which depends sensitively on self-consistency is the imaginary part of Σ . If, in Eqs. (1), the entire self-energy is replaced by a constant imaginary piece Γ , the resulting equation for the single-particle Γ reduces to that found in Refs. 5. Here, the self-consistency in the equation for Γ emerges naturally. Our numerical solutions for the inverse quasiparticle lifetime are compared with various analytical expressions in the inset of Fig. 1. Curve (1) corresponds to the perturbation result⁵ $\Gamma^{(1)} = (T/4\epsilon_F\tau) \ln[16D\kappa^2(\epsilon_F\tau)^2/T]$. Curve (2) is a plot of the self-consistently determined⁵ $\Gamma^{(2)} = (T/4\epsilon_F\tau) \ln[D\kappa^2 T/(\Gamma^{(2)})^2]$ and curve (3) includes Γ/T corrections to $\Gamma^{(2)}$ resulting from the solution of $\Gamma^{(3)} = (T/2\pi\epsilon_F\tau) (\tan^{-1} T/\Gamma^{(3)}) \ln[D\kappa^2 T/(\Gamma^{(3)})^2]$. Here κ is the usual 2D screening length.⁴ For moderate to large disorder our numerical results for Γ (evaluated at $\omega=0$ and shown by the squares) differ from all of the above primarily because of renormalizations due to $\text{Re}Z$. This effect leads to a factor-of-2 discrepancy for our most disordered system ($\epsilon_F\tau=5$). For this disorder the suppression of the magnitude of Γ is accompanied by considerable frequency structure in the real part (as well as the imaginary part) of Z . The frequency dependence of $\text{Re}Z$ is shown in Fig. 1(a) for $\epsilon_F\tau=5$. [The actual curve corresponds to a superconducting system but $\text{Re}Z(\omega)$ is found to be relatively unaffected by the superconducting order.] It should be stressed that the magnitude of the deviation of $Z(\omega)$ from 1.0 is considerable and $Z(\omega) - 1$ assumes values comparable to those in strong-coupling superconductors. However, unlike the

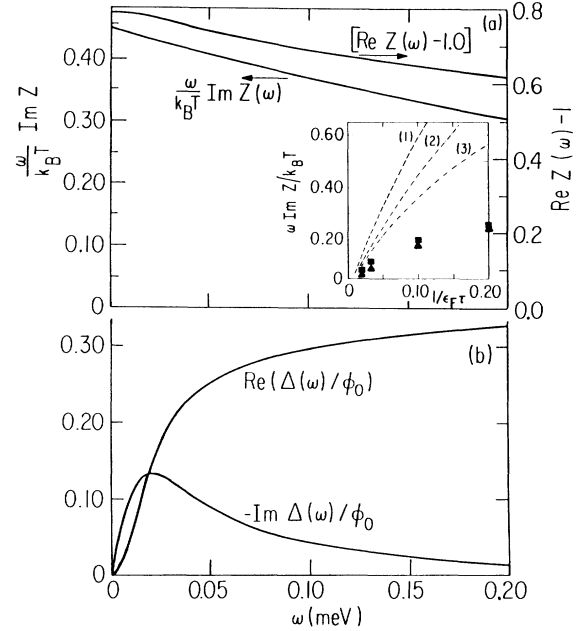


FIG. 1. Frequency dependence of the renormalization function $Z(\omega)$ and gap parameters $\Delta(\omega)$ at $T=1$ K for $\epsilon_F\tau=5.0$. Here ϕ_0 is the phonon contribution to the gap. Inset: The scattering rate at $\omega=0$ vs $1/\epsilon_F\tau$. Dashed lines, defined in the text, represent analytical approximations which are compared with our numerical results for normal (squares) and superconducting (triangles) samples.

strong-coupling superconductors, $\text{Re}Z(\omega) - 1$ varies considerably over an extremely narrow range of low frequencies.

This frequency variation in $\text{Re}Z(\omega)$ is mirrored by structure on a similar scale in the normal density of states. We note that to leading order in $(\epsilon_F\tau)^{-1}$ the normal density of states derived from Eqs. (1) reduces to that obtained elsewhere.⁷ For larger disorder the normal-state self-energy required numerical solution. We found that it was important to include the full frequency dependence of the inelastic lifetime in order to compute the resulting normal-state density of states at $T=1.0$ K, which is shown in the inset of Fig. 2 for various $\epsilon_F\tau$ with $\epsilon_F=10^4$ K. These curves, which clearly show the large depression in $N_n(\omega)$ from the clean value, can be compared to the perturbation results (see dashed lines). For larger disorder, a flattening of the curves near $\omega=0$ occurs relative to the perturbation results. This arises because for high disorder the logarithmic divergence in the density of states is smeared out by inelastic processes rather than by thermal fluctuations. It is important to note that in the present calculation the depression in $N_n(\omega)$ is found to grow more slowly with disorder than the perturbation-theory prediction.

When compared to the normal state, Z and Z_3 are modified as a result of the superconducting pairing. The

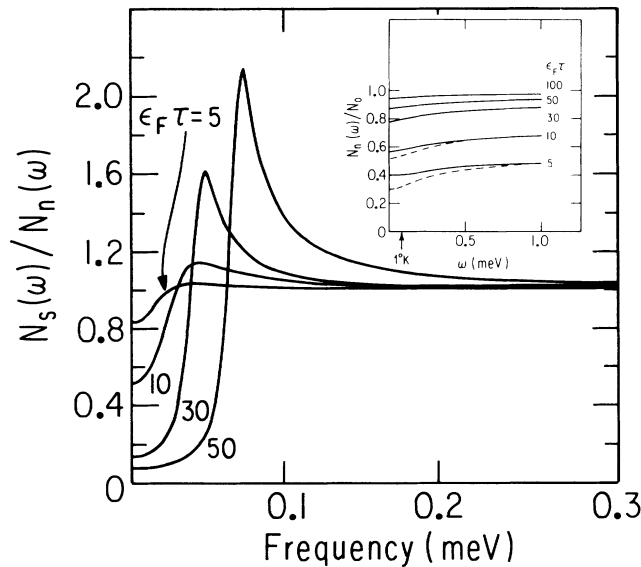


FIG. 2. Density of states in the superconducting state at $T=1$ K for various $\epsilon_F\tau$ values. Here $T_c=1.2$ K. Inset: The normal-state density of states for the same parameters. The dashed lines are perturbation results.

most dramatic effect is in $\text{Im}Z$ because it is most sensitive to the behavior near the Fermi level. The reduction of the number of states at low energy by the Cooper pairing leads to an increased quasiparticle lifetime in the superconducting state. Presumably this will have a number of interesting experimental consequences. The triangles in the inset of Fig. 1 indicate the values of the inverse quasiparticle lifetime at $\omega=0$ in the superconducting state. The comparison with the normal-state values (squares) shows the degree of suppression of the scattering rate. Here the Debye frequency and the electron-phonon coupling were adjusted to give a superconducting gap in the clean limit of 1 K. For $\epsilon_F\tau=5$, Fig. 1(a) shows the frequency dependence of the inelastic scattering rate in the superconducting system. This frequency dependence is comparable to that observed in $\text{Re}Z(\omega)$.

For this same moderately disordered system we have found that the inelastic-scattering rate gives rise to gapless superconductivity. This derives in large part from the significant suppression of the order parameter, as a result of renormalization due to $\text{Re}Z$. At $T=1$ K, we find $\Gamma \sim 0.22k_B T$ (see Fig. 1) which is roughly equal to the order parameter (also suppressed by $\text{Re}Z$) and is thus sufficient to give rise to gaplessness. *It should be stressed that even when the ratio of these two quantities is as low as 0.1 ($\epsilon_F\tau=50$) we will see some degree of gaplessness (see Fig. 2) unlike the situation in magnetically dirty superconductors.* This is due to the fact that

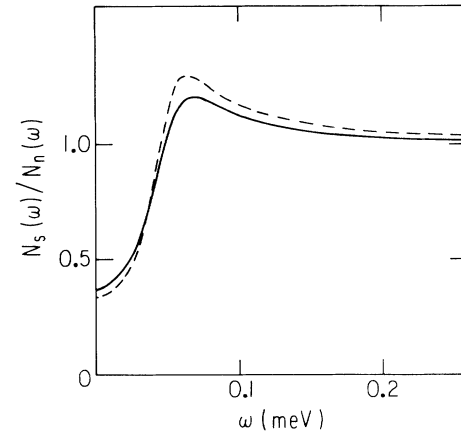


FIG. 3. Comparison of phenomenological pair-breaking model (see text) for $N_s(\omega)$ (dashed curve) with full numerical results (solid curve).

the pair-breaking mechanism is inelastic. The frequency structure and values of the complex gap parameter $\Delta(\omega) = \Phi(\omega)/Z(\omega)$ are shown in Fig. 1(b). Note that the maximum in $\text{Im}\Delta(\omega)$ occurs at frequency ω^{max} corresponding to the inverse of the renormalized quasiparticle lifetime $\omega^{\text{max}} \sim \omega \text{Im}Z/\text{Re}Z|_{\omega^{\text{max}}}$. In addition, $\text{Re}\Delta(\omega)$ which vanishes with $\omega \rightarrow 0$ as ω^2 is clearly suppressed even at large ω relative to the expected value of $\sim k_B T_c$ for a clean system.

In Fig. 2 is plotted the superconducting density of states for various $\epsilon_F\tau$ ranging from 50 to 5. Note that the characteristic peak in the density of states occurs below the clean gap value, in large part because of the reduction of the gap by a factor $\text{Re}Z$. As the disorder increases the density of states rapidly fills in at low frequency. At high disorder there is a slight dip just above the renormalized gap frequency. This arises from a competition between the normal-state reduction in $N_n(\omega)$ and the usual increase in $N_s(\omega)$ just above the gap frequency.

Dynes *et al.*³ have reported gaplessness in granular aluminum samples, the onset of which correlates well with other indicators of strong localization. The present results for $N_s(\omega)$ shown in Fig. 2 contain the gross features of the data in Ref. 3. The authors proposed a simple one-parameter pair-breaking formula for $N_s(\omega) = N_n(0)\text{Re}(\omega+i\gamma)[(\omega+i\gamma)^2+\Delta_0^2]^{-1/2}$ where γ represents the broadening of the single-particle states due to inelastic scattering and Δ_0 is the superconducting gap. This phenomenological form (dashed line) is compared with our numerical results in Fig. 3. To make the two curves as similar as possible we chose the gap value Δ_0 to be such that the peaks in the two curves for $N_s(\omega)$ occur at the same position. The inverse lifetime was chosen to be $\gamma \equiv \omega \text{Im}Z(\omega)/\text{Re}Z(\omega)|_{\Delta_0}$ which was evaluated by

Eq. (1). The differences in the two curves, which we view as important, arise primarily from the frequency structure in $\Delta(\omega) \equiv \Phi/\text{Re}Z(\omega)$ deriving from $Z(\omega)$. Thus these differences contain information about the dynamics of the Coulomb interaction. While ours represents a fully microscopic—as distinct from a phenomenological—theory, the results presented here should not be used to describe quantitatively the tunneling data of Ref. 3, since much of the data presented there are in the strongly localized regime and for three-dimensional (3D) samples. The present approach can be extended to this case by the introduction of an energy- and scale-dependent diffusion constant D following Ref. 2. This should lead to quantitative but not qualitative changes. Additionally, in order to probe the frequency structure associated with the Coulomb interaction and thus to quantify the differences between the two curves in Fig. 3, more detailed and systematic experiments are also needed. If we interpret the factor $\epsilon_F\tau$ as the resistivity divided by the Mott resistivity, in the most disordered samples of Ref. 3 one finds from Eqs. (1) an inelastic-scattering inverse lifetime of 0.02 meV which is of the correct magnitude as deduced from these tunneling experiments.

While detailed future analyses of the frequency structure in $N_s(\omega)$ can be useful in elucidating the nature of the dynamical Coulomb interaction, even more important are temperature-dependent studies. Because the inelastic scattering is much weaker, the superconducting density of states at low T more closely resembles that of a clean superconductor. This effect, which is seen in our numerical calculations, is a very important signature of Coulomb-induced structure in $N_s(\omega)$ and clearly should be verified experimentally.

In summary, there is an intimate relationship between anomalies observed in the normal and superconducting states in highly disordered superconductors. This results from an interesting interplay between the superconductivity and *dynamical* Coulomb effects. As one consequence, the inelastic-scattering lifetime significantly af-

fects the superconductivity, while at the same time it is itself modified by the onset of the pairing. The latter effect should be studied in future transport measurements, whereas the former is already evident in superconducting tunneling. Clearly, experimental studies *within* the superconducting state may prove to be among the most useful probes of the interplay of Coulomb interactions and disorder.

We thank Bruce Patton, J. M. B. dos Santos, R. C. Dynes, and T. P. Orlando for useful discussions. This work was supported by the National Science Foundation through Grant No. DMR-81-15618, the National Science Foundation Materials Research Laboratories Program, through Grant No. NSF-DMR-16892, and the Exxon Educational Foundation.

^(a)Permanent address: Laboratory for Atomic and Solid State Physics, Cornell University, Ithaca, NY 14853.

^(b)Permanent address: Brookhaven National Laboratory, Upton, NY 11973.

¹S. Maekawa and H. Fukuyama, J. Phys. Soc. Jpn. **50**, 2516 (1981), and **51**, 1380 (1982); H. Takagi and Y. Kuroda, Solid State Commun. **41**, 653 (1982).

²P. W. Anderson, K. A. Muttalib, and T. V. Ramakrishnan, Phys. Rev. B **28**, 117 (1983).

³R. C. Dynes, J. P. Garno, G. B. Hertel, and T. P. Orlando, Phys. Rev. Lett. **53**, 2437 (1984).

⁴E. Abrahams, P. W. Anderson, P. A. Lee, and T. V. Ramakrishnan, Phys. Rev. B **24**, 6783 (1982). Among the first applications of the exact-eigenfunction approach to highly disordered superconductors is that of B. Keck and A. Schmidt, J. Low Temp. Phys. **24**, 611 (1976).

⁵H. Fukuyama and E. Abrahams, Phys. Rev. B **27**, 5976 (1983); J. M. B. Lopes dos Santos, Phys. Rev. B **28**, 1189 (1984).

⁶A. Schmid, Z. Phys. **259**, 421 (1973); K. A. Muttalib, Ph.D. thesis, Princeton University, 1982 (unpublished).

⁷B. L. Al'tshuler and A. G. Aronov, Pis'ma Zh. Eksp. Teor. Fiz. **30**, 482 (1979) [Sov. Phys. JETP Lett. **30**, 514 (1979)].